

Investigation of Ionization and Coupling Mechanisms for Pivaloylacetanilide Yellow Couplers Bearing *o*-Sulfonamidophenoxy Coupling-Off Groups.

Michael P. Youngblood, Thomas R. Welter, and Faraj Abu-Hasanayn
Eastman Kodak Company, Rochester, New York USA

Abstract

For pivaloylacetanilide yellow couplers bearing *o*-sulfonamidophenoxy coupling-off group (e.g., Cpd 2 in Table I), there are two ionizable protons: one from the β-dicarbonyl group (the coupling site) and another from the sulfonamide function on the coupling-off group (COG). By measuring the UV spectra of coupler solutions in phosphate buffers ranging in pH from 5 to 12, we determined the pK_a values of the series of couplers shown in Table I. Figure 1 shows examples of the absorbance vs. pH data used in the pK_a determinations. The curves in Fig. 1 are nonlinear regression fits to the data points using Eq. 1 for the monoprotic couplers or Eq. 2 for the diprotic couplers. In these equations, A_i (i = 1, 2, or3) is the absorbance due to the

$$A = \frac{A_1[H^+] + A_2K_{a1}}{[H^+] + K_{a1}} \quad (1)$$

$$A = \frac{A_1[H^+]^2 + A_2K_{a1}[H^+] + A_3K_{a1}K_{a2}}{[H^+]^2 + K_{a1}[H^+] + K_{a1}K_{a2}} \quad (2)$$

un-ionized, mono-ionized or di-ionized coupler species when 100% of the coupler is in each of these respective states of ionization (equivalent to $\varepsilon_i bc$ in the conventional Beer's Law notation). In the nonlinear regressions, A_i and K_a were regression parameters fit to experimentally measured pH and absorbance values. The wavelength for each determination was chosen to give the largest total absorbance change. Each diprotic coupler exhibits two characteristic absorbance changes, ΔA_1, and ΔA_2, defined as A_2-A_1 and A_3-A_2.

In Fig. 1, the single absorbance change, ΔA, that occurs upon ionization of the monoprotic coupler Cpd 1 is 2.81, quite similar to 2.77, the total of the two absorbance changes, $\Delta A_1 + \Delta A_2$, that accompany the two ionizations of Cpd 2. The ionization of the benzyl-blocked CPD 2 COG gives a much smaller absorbance change: 0.434 at 310 nm, where its ΔA is largest, but even smaller in the wavelength range where the coupler pK_as are measured. Inspection of Table I reveals that $\Delta A_1 + \Delta A_2$ for full ionization of any of the diprotic couplers and the single ΔA for ionization of the monoprotic couplers Cpd 1 and Cpd 4, are similar and substantially larger than that for the the benzyl-blocked Cpd 2 COG. Also, the values of ΔA_1 and ΔA_2 for the diprotic couplers vary significantly through the series, even though the total absorbance changes are all quite similar.

Given the curves in Fig. 1 and the ΔA values in Table I, it is reasonable that the absorbance changes reflect mainly the amount of β–dicarbonyl ionization that occurs at each measured pK_a. If so, the results in Table I suggest the involvement of microscopic ionization equilibria for the diprotic couplers. That is, the first macroscopic ionization (pK_{a1}) results in partial ionization of the β–dicarbonyl site and the sulfonamide site. The microscopic equilibria are illustrated in Scheme 1. The existence of microscopic equilibria would explain why $\Delta A_1 + \Delta A_2$ is relatively constant even while the values of ΔA_1 and ΔA_2 vary greatly among the couplers. Large ΔA_1 values occur when the first ionization involves mainly β–dicarbonyl ionization, while smaller values of ΔA_1 mean that sulfonamide ionization predominates. ΔA_2 reflects mainly the amount of β–dicarbonyl ionization that occurs at the second macroscopic pK_a, and this amount is equal to the amount of of sulfonamide ionization that occurs at the first macroscopic pK_a, as required by mass balance. Hence the ratio $\Delta A_2/\Delta A1$ represents an approximation of K_{11} in Scheme 1.

The coupling kinetics of the couplers in Table I with quinone diimine (D_{ox}) also reflect the existence of the proposed microscopic equilibria. The dependence of log k_c on pH, where k_c is the second-order coupling rate constant, is shown in Fig. 4 for Cpd 2 and Cpd 4. These couplers differ only by a -H (CPD 2) vs a -CH_3 (CPD 4) substituent at the sulfonamide nitrogen in the COG. The presence of the ionizable sulfonamide -NH in Cpd 2, and its absence in Cpd 4 have a large effect on the pH profiles for these two couplers. There are two distinct and significant breaks in the profile for Cpd 2, each near the measured pK_as, and only

one in the case of Cpd 4, again near the measured pK_a. The behavior of Cpd 2 is qualitatively consistent with the microscopic equilibria hypothesis: The two breaks in the pH profile are observed for all the diprotic couplers in Table I and can be explained by successive partial ionizations of the β–dicarbonyl coupling site. Nonlinear regression of data such as that in Figs. 1 and 2 affords the determination of macroscopic and microscopic equilibrium constants and bimolecular rate constants for singly and doubly ionized couplers. These are summarized in Table III.

Fig. 1. Spectrophotometric pK_a Determinations

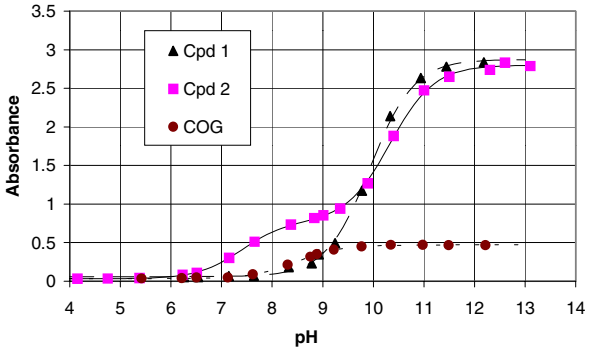

Fig. 2. pH Profiles for Coupling Kinetics of Cpd 2 and Cpd 4

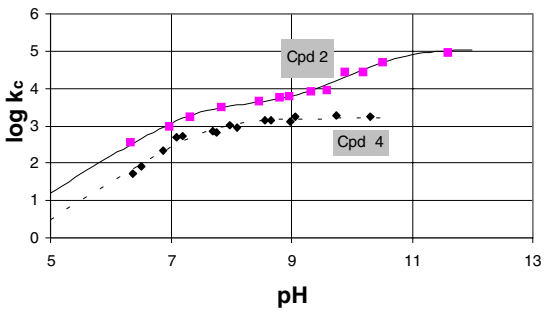

Table I. Coupling-Off Group Variation with Pivaloylacetanilide Yellow Couplers: Results of Spectrophotometric pK_a Determination

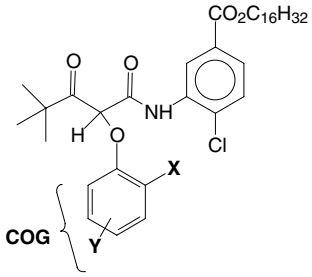

Coupler	X	Y	pK_{a1} [a]	pK_{a2} [a]	λ (nm)	ΔA_1	ΔA_2
Cpd 1	COG = H	COG = H	9.92	-	324	2.812	-
Cpd 2	$NHSO_2CH_3$	4-SO_2CH_3	7.39	10.33	340	0.742	2.026
COG[b]	$NHSO_2CH_3$	4-SO_2CH_3	8.48	-	310	0.434	-
Cpd 3	SO_2CH_3	4-$NHSO_2CH_3$	8.08	9.84	340	1.564	1.508
Cpd 4	$N(CH_3)SO_2CH_3$	4-SO_2CH_3	8.36	-	320	2.743	-
Cpd 5	$NHSO_2CH_3$	4-$SO_2C_2H_5$	7.54	10.42	340	0.659	1.708
Cpd 6	$NHSO_2C_6H_5$	4-$SO_2C_2H_5$	7.17	10.78	340	0.321	2.304
Cpd 7	$NHSO_2(C_6H_5$-4-$NO_2)$	4-$SO_2C_2H_5$	5.81	10.75	340	0.382	2.353
Cpd 8	$NHSO_2CH_3$	H	8.94	12.02	320	2.315	0.552
Cpd 9	$NHSO_2C_6H_5$	H	8.86	12.05	320	1.315	1.627
Cpd 10	$NHSO_2(C_6H_5$-4-$NO_2)$	H	7.55	12.05	320	0.175	2.531
Cpd 11	$NHSO_2CH_3$	4-CO_2CH_3	8.17	11.05	340	1.388	1.331
Cpd 12	$NHSO_2CH_3$	5-CO_2CH_3	7.58	11.67	340	1.048	1.686

[a] pK_a determined at T = 25°C, μ = 0.375

[b] Benzyl-blocked COG of Cpd 2: $C_6H_5CH_2OC_6H_5(2$-$NHSO_2CH_3$-4-$SO_2CH_3)$

Scheme 1. Microscopic Equilibria

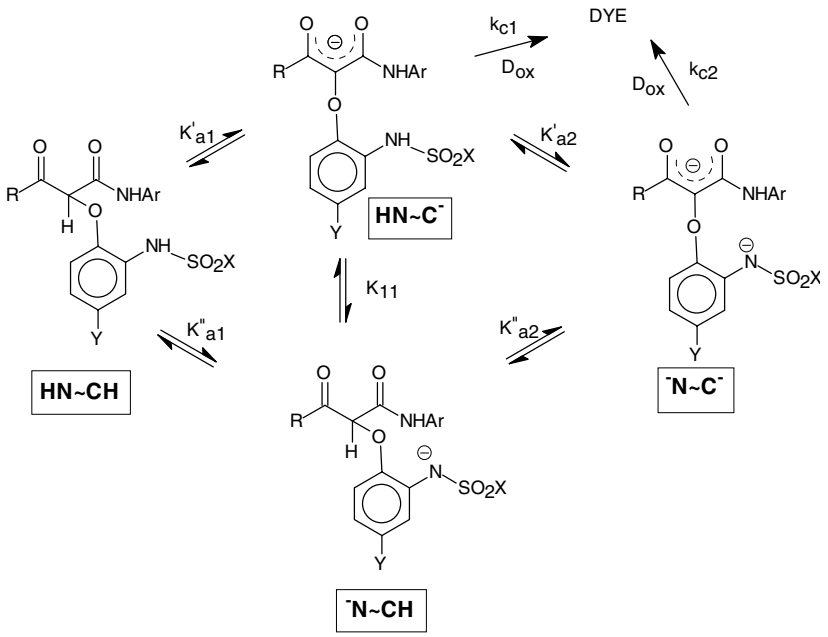

Table II. Macroscopic and Microscopic pKa and Rate Constant Summary

	Macroscopic Constants				Estimated Microscopic Constants						
Coupler	pK_{a1}	pK_{a2}	log k_1	log k_2	K_{11}	pK'a1	pK"a1	pK'a2	pK"a2	log k_{c1}	log k_{c2}
Cpd 2	7.39	10.33	3.60	5.05	2.73	7.96	7.53	9.76	10.19	4.17	5.05
Cpd 3	8.08	9.84	3.00	3.31	1.00	8.38	8.38	9.54	9.54	3.30	3.31
Cpd 5	7.54	10.42	3.57	5.27	2.59	8.10	7.68	9.86	10.28	4.13	5.27
Cpd 6	7.17	10.78	3.13	5.55	7.18	8.08	7.23	9.87	10.72	4.04	5.55
Cpd 7	5.81	10.75	2.16	5.26	6.16	6.66	5.88	9.90	10.68	3.01	5.26
Cpd 8	8.94	12.02	4.07	5.56	0.24	9.03	9.66	11.93	11.30	4.16	5.56
Cpd 9	8.86	12.05	3.80	5.47	1.24	9.21	9.12	11.70	11.79	4.15	5.47
Cpd 10	7.53	12.05	3.27	5.60	14.46	8.72	7.56	10.86	12.02	4.46	5.60
Cpd 11	8.17	11.05	3.64	5.37	0.96	8.46	8.48	10.76	10.74	3.93	5.37
Cpd 12	7.58	11.67	3.26	5.16	1.61	8.00	7.79	11.25	11.46	3.68	5.16

Biography

Michael Youngblood received his B.S. degree in Chemistry from the University of Georgia in 1973 and a Ph.D. in Analytical Chemistry from Purdue University in 1979. Since 1979 he has worked in the Research Laboratories at Eastman Kodak company in Rochester, NY. His work has focused primarily on the kinetics and mechanisms of chemical reactions of photographic importance and the application of mechanistic understanding to improved photographic products.